NASA TECHNICAL NOTE

NASA TN D-7584

NASA TN D-7584

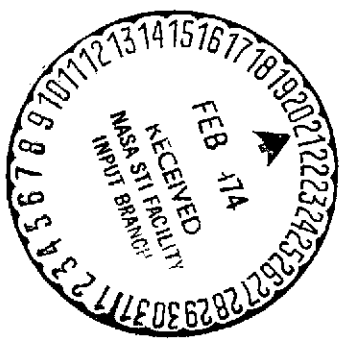

HEAT TRANSFER CHARACTERISTICS OF AN EMERGENT STRAND

by William Emile Simon, Larry Claude Witte, and Pat Garner Hedgcoxe

Lyndon B. Johnson Space Center
Houston, Texas 77058

NATIONAL AERONAUTICS AND SPACE ADMINISTRATION • WASHINGTON, D. C. • FEBRUARY 1974

1. Report No.	2. Government Accession No.	3. Recipient's Catalog No.
D- 7584		

4. Title and Subtitle	5. Report Date
HEAT TRANSFER CHARACTERISTICS OF AN EMERGENT STRAND	February 1974
	6. Performing Organization Code

7. Author(s)	8. Performing Organization Report No.
William Emile Simon, JSC, and Larry Claude Witte and Pat Garner Hedgcoxe, University of Houston	JSC S-362
	10. Work Unit No.
9. Performing Organization Name and Address	981-10-00-00-72
Lyndon B. Johnson Space Center Houston, Texas 77058	11. Contract or Grant No.
	13. Type of Report and Period Covered
12. Sponsoring Agency Name and Address	Technical Note
National Aeronautics and Space Administration Washington, D.C. 20546	14. Sponsoring Agency Code

15. Supplementary Notes

16. Abstract

A mathematical model is developed to describe the heat transfer characteristics of a hot strand emerging into a surrounding coolant. A stable strand of constant efflux velocity is analyzed, with a constant (average) heat transfer coefficient on the sides and leading surface of the strand. After developing a suitable governing equation to provide an adequate description of the physical system, the dimensionless governing equation is solved with Laplace transform methods. The solution yields the temperature within the strand as a function of axial distance and time. Generalized results for a wide range of parameters are presented, and the relationship of the results and experimental observations is discussed.

17. Key Words (Suggested by Author(s))	18. Distribution Statement
*Heat Transfer *Film Boiling *Heat Transmission *Heat Transfer Coefficients *Liquid-Liquid Interfaces *Liquid-Vapor Interfaces	Cat. 33

19. Security Classif. (of this report)	20. Security Classif. (of this page)	21. No. of Pages	22. Price
None	None	39 ~~38~~	$3.00

*For sale by the National Technical Information Service, Springfield, Virginia 22151

CONTENTS

TABLE

FIGURES

HEAT TRANSFER CHARACTERISTICS OF AN EMERGENT STRAND

By William Emile Simon, Larry Claude Witte,* and Pat Garner Hedgcoxe*
Lyndon B. Johnson Space Center

SUMMARY

The results of an analysis of the heat transfer characteristics of a hot strand emerging into a surrounding cooler fluid are presented. The analysis is for a stable strand of constant efflux velocity, with a constant heat transfer coefficient on the leading surface and strand sides. A dimensionless governing equation is derived and solved by Laplace transform methods. The equation provides a description of the variation of temperature within the strand with axial distance and time. Following a discussion of computational aspects of the solution, generalized results are presented for a wide range of parameters. A discussion of the relationship of the generalized results and experimental observations is given.

INTRODUCTION

When a hot emergent strand of an incompressible fluid or semisolid material penetrates a cool liquid bath, heat is lost rapidly from the sides and leading edge of the strand. If the strand is a hot molten material, explosive vapor formation may occur, caused by fragmentation of the molten material (ref. 1). Conversely, the strand may be of a metal or a fiber in its plastic deformation region, being extruded and quenched simultaneously.

In the area of nuclear reactor safety, an over-temperature excursion within a reactor can cause overheating of the fuel elements, possibly to the point of becoming molten, while also generating fission gases and increasing the pressure level inside the fuel elements. When this happens, the temperature of the cladding that surrounds the fuel element rises, ultimately causing a cladding rupture that can result in the release of a high-temperature molten jet stream into the surrounding coolant. Film boiling begins immediately on the exposed material and continues until the stream cools sufficiently for the system to enter the transition and subsequent nucleate boiling regimes. The violent nature of transition and nucleate boiling quickly overcomes the surface tension forces holding the molten metal together and tears the molten mass into smaller globules. The process sets off a thermal chain reaction because, as more exposed surface area is provided as a result of disintegration, the heat transfer

*University of Houston, Houston, Texas.

increases, causing further disintegration by nucleate boiling. The fragmentation process continues until, in some cases, the molten fluid is reduced to a very fine powder. If the time to transition boiling can be predicted, information can be obtained on the amount of energy released up to this point and on the delay times involved in the vapor explosion process.

The transportation of liquefied natural gas (LNG) by large oceangoing vessels is another application of the processes analyzed in this report. A leak in the hull of an LNG vessel could allow seawater to penetrate the LNG. Because of the large temperature difference between the two fluids, the LNG would begin to boil off the sides of the seawater stream, resulting in a phenomenon analogous to the analysis of this report.

Another application is in the metal-forming industry, in which it is often necessary to form metal bars by means of an extrusion or, perhaps, a rolling process. A closely related situation concerns a metal wire being drawn from a die, or a monofilament fiber being drawn from a spinneret (melt spinning). As indicated in reference 2, only in the recent past has melt spinning been the subject of fundamental research. If the cooling behavior of a wire (or billet) being extruded could be predicted, it might be possible to combine the metal-forming and the heat-treating processes into one.

The applications just described are the ones that provided the motivation for this study. In these applications, a fundamental understanding of basic heat transfer within the strand is essential. Many parameters govern the thermal performance of the strand. In this report, a mathematical model is developed and the governing equation is derived to describe the heat transfer characteristics of the strand. The governing equation is then solved for the temperature within the strand as a function of axial distance and time. Finally, a computer program is used to vary the parameters governing the heat transfer process and to determine the degree of influence of each. (The applicability of this analysis to emerging liquid strands or streams is very limited because, by assuming a stable strand geometry, the complex fluid dynamic interactions between the strand and the surrounding cooler fluid are neglected.)

For this report, a stable, one-dimensional, circular strand of constant efflux velocity is assumed, with a constant (average) heat transfer coefficient on the sides and leading surface of the strand. However, the heat transfer coefficient on the end of the strand need not be equal to that of the sides. For convenience, the cylindrical body is referred to as a strand, whether it is a wire, billet, fiber, molten jet, or other form.

The approach to the heat transfer solution is similar to that of the classical fin heat transfer analysis (ref. 3), but the problem is complicated by the fact that the strand is in motion, while at the same time it is always physically connected to the fixed reservoir, resulting in a constantly changing geometry. Therefore, a departure from classical techniques is needed to arrive at a solution to this particular problem for the short times of interest in some applications (e.g., the vapor explosion problem). For large times, the solution is analogous to the well-known semi-infinite rod problem.

As an aid to the reader, where necessary the original units of measure have been converted to the equivalent value in the Système International d'Unités (SI). The SI units are written first, and the original units are written parenthetically thereafter.

SYMBOLS

Bi	Biot number, hr/k
Bi_e	Biot number at the end, $h_e r/k$
c_p	specific heat of strand material
Fo	Fourier modulus, $\alpha\tau/r^2$
Fo*	time to steady state
h	heat transfer coefficient on strand sides
k	thermal conductivity of strand material
Pe	Peclet number, rU/α
Pr	Prandtl number, $c_p\mu/k$
q_{gen}	heat generated within elemental volume
q_i	heat entering elemental volume
q_ℓ	heat lost from strand sides
q_o	heat leaving elemental volume
q_s	heat stored in elemental volume
q"	local heat transfer rate per unit area
r	strand radius
Re	Reynolds number, $rU\rho/\mu$
s	transform variable
s_1, s_2	quadratic roots
T	temperature
T_o	reservoir temperature
T_∞	coolant temperature

U	strand efflux velocity
u	Heaviside unit function
x	coordinate position, distance from the entrance
z	function, defined in equation (B9)
α	thermal diffusivity of strand material
γ	dimensional parameter, 2h/kr
η	dimensionless distance, ξ/r
η^*	steady-state distance
θ	dimensionless temperature
μ	absolute viscosity of strand material
ξ	position coordinate, distance from the leading edge
ρ	density of strand material
τ	time

FORMULATION OF THE ANALYTICAL MODEL

To begin the analysis, consideration first is given to the flow of a round axisymmetric strand in the region of stable film boiling with constant efflux of the molten material or strand. As opposed to the analysis of Schlichting (ref. 4) for a jet that mixes with the surrounding fluid, in this analysis a stable jet or strand is assumed, with no mixing of the strand material and the coolant. Neglecting leading-edge deformation (ref. 5 is suggested as a starting point for analyzing the effects of velocity retardation and deformation), the physical process can then be modeled by a blunt-edged strand of radius r penetrating the coolant as shown in figure 1. A vapor film forms at the leading surface and continues toward the wall, completely engulfing the strand sides. At any given position, the vapor film thickness will grow with time, always being thinnest at the leading edge. Because the film boiling process greatly reduces skin friction at the strand surface (refs. 6 and 7), velocity gradients within the molten material are neglected. In addition, because of the high thermal conductivity of liquid metals and the small radii of practical interest, radial temperature gradients within the strand are neglected. In summary, the following assumptions are made concerning the problem: a stable axisymmetric strand at constant velocity, radial temperature gradients neglected, and constant heat transfer coefficient.

When a hot or molten strand emerges into a region of cool liquid, three factors are of primary importance: the fluid-dynamic characteristics of the strand system; the boiling of the coolant; and the cooling and solidification of the molten material. For the case of a fiber or strand being drawn through a coolant medium, boiling may or may

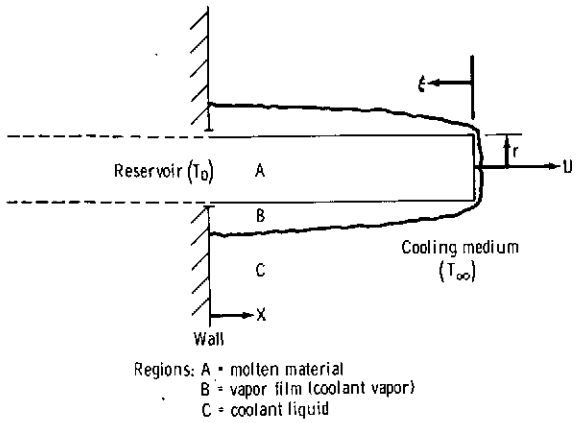

Figure 1.- Emergent strand penetrating surrounding coolant.

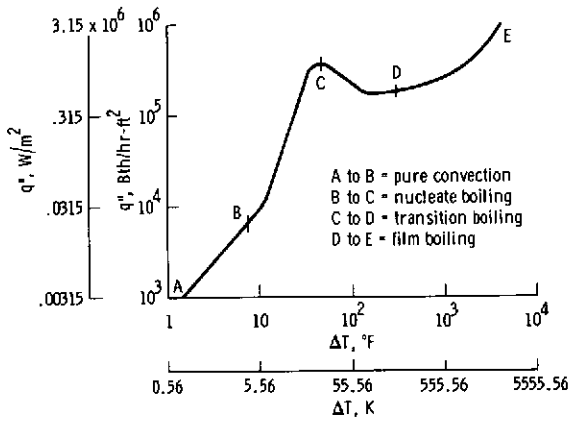

Figure 2.- Boiling of water at 373° K (212° F) on an electrically heated platinum wire, showing various boiling regimes.

not be involved, and the cooling process is simpler than that of the molten material because no solidification is involved.

For the molten strand problem, it is assumed that, when the strand first emerges from the opening, stable film boiling with strong radiation effects occurs (ref. 8). As the strand travels downstream, cooling as it goes, it eventually reaches a temperature at which stable film boiling exists without appreciable radiation effects. Further cooling results in a region of partial nucleate boiling and unstable film boiling. Next comes the nucleate boiling regime; if the strand does not disintegrate, pure convection will follow. The various heat transfer regimes are shown in figure 2 (ref. 9). Experimental work concerning vapor explosion indicates that under certain conditions the molten material will disintegrate violently somewhere in the region of nucleate boiling. The disintegration and subsequent solidification process is very complicated. Disintegration produces a rapid increase in heat transfer area that increases the heat flux, thus causing a self-propagating effect and hastening the heat transfer process even further. In addition to the various heat transfer regimes, the velocity regions of laminar and turbulent flow are also important for both the molten material or fiber and the cooler liquid (liquid and vapor regions).

To determine the heat transfer coefficient governing the removal of heat from the surface of the strand, the equations of heat, mass, and momentum transfer must be accompanied by appropriate boundary conditions for each heat transfer and velocity region, and further boundary conditions connecting the various regions must be satisfied. If the heat transfer coefficient is known beforehand or if an average coefficient is used, the analysis is concentrated on the heat transfer within the hot material, which is the case for this report. More information on the calculation of the heat transfer coefficient is given in appendix A. (Since the heat transfer coefficient is treated parametrically in the main body of this report, this appendix is therefore an independent entity and can be considered entirely separate from the report. The purpose of appendix A is to merely suggest one possible approach to the extremely difficult problem of computing the heat transfer coefficient.)

To derive the governing differential equation of the strand system, consider first the elemental cross section of the strand shown in figure 3. In the general case, h is the overall coefficient of heat transfer for convection, radiation, and film boiling. The quantities q_i and q_o are those of heat transfer into and out of the elemental volume. Heat stored within the element is denoted by q_s; q_ℓ is the heat lost off the sides because of convection and so forth. It is assumed that the temperature of the surrounding coolant T_∞ remains constant.

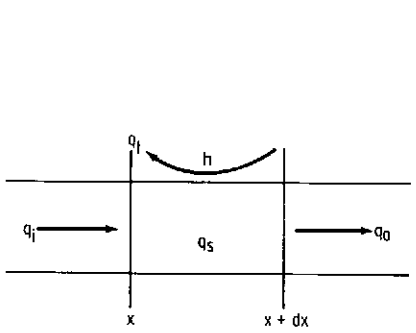

Figure 3.- Elemental volume of strand showing energy balance.

It is convenient to translate the coordinate axes to a moving coordinate system at the leading edge of the strand. This translation is accomplished by means of the transformation

$$\xi \equiv U\tau - x \tag{1}$$

where ξ is the position coordinate, distance from the leading edge; U is jet efflux velocity; τ is time; and x is the coordinate position, distance from the entrance. At all times, $\xi \geq 0$. The moving coordinate system is also shown in figure 1. An elemental heat balance including heat conducted into and out of the element, heat lost from the sides of the element, and net heat accumulation by the element yields the basic equation

$$\frac{\partial^2 \theta}{\partial \xi^2} - \gamma\theta = \frac{1}{\alpha}\frac{\partial \theta}{\partial \tau} \tag{2}$$

where $\gamma = 2h/kr$, a dimensional parameter; α is the thermal diffusivity of the strand material; and the dimensionless temperature θ is defined as

$$\theta(\tau) \equiv \frac{T - T_\infty}{T_o - T_\infty} \tag{3}$$

where T is the temperature of the strand material and T_o is the reservoir temperature.

For equation (2) to apply in both regions (outside the wall on the strand surface and inside the reservoir), the Heaviside unit function u (ref. 10) is introduced.

$$u\left[\frac{\alpha}{r^2}\left(\tau - \frac{\xi}{U}\right)\right] = \begin{cases} 0, & \tau < \frac{\xi}{U} \\ 1, & \tau \geq \frac{\xi}{U} \end{cases} \tag{4}$$

If the actual temperature gradient at the entrance is modified so that $\theta = \theta_o \equiv 1$ at $\xi = U\tau$, then multiplying the heat transfer coefficient γ in equation (2) by $u[\frac{\alpha}{r^2}(\tau - \frac{\xi}{U})]$ results in the following modification of equation (2):

$$\frac{\partial^2\theta}{\partial\xi^2} - \gamma u\left[\frac{\alpha}{r^2}\left(\tau - \frac{\xi}{U}\right)\right]\theta = \frac{1}{\alpha}\frac{\partial\theta}{\partial\tau} \tag{5}$$

In this formulation, when $\xi \leq U\tau$, heat is transferred from the sides at the rate γ; when $\xi > U\tau$, no heat is allowed to flow from the sides of the strand within the reservoir (dotted lines in fig. 1).

In seeking a closed-form analytical solution, it is apparent that in the transformed coordinate system, in which the position coordinate ξ is always greater than or equal to zero, the governing equation is particularly suited to the Laplace transform method of solution. However, solution of equation (5) by the Laplace transform method leads to a more complicated equation, and another approach is therefore taken.

The energy balance equation rewritten in its most general form is $q_i - q_o + q_{gen} = q_s + q_\ell$ (where the heat generation term q_{gen} is zero outside the wall). However, inside the wall, because the term q_ℓ dictates that heat still is being lost from the sides of the strand, an equal and opposite amount of heat must be generated within the strand to replenish the heat lost. This make-up quantity of heat can be expressed as

$$q_{gen} = 2\pi r h\, d\xi\left(T_o - T_\infty\right)\left\{1 - u\left[\frac{\alpha}{r^2}\left(\tau - \frac{\xi}{U}\right)\right]\right\} \tag{6}$$

because the strand is essentially at T_o inside the reservoir. The governing equation for this physical model then becomes

$$\frac{\partial^2\theta}{\partial\xi^2} - \gamma\theta = \frac{1}{\alpha}\frac{\partial\theta}{\partial\tau} - \gamma\theta_o\left\{1 - u\left[\frac{\alpha}{r^2}\left(\tau - \frac{\xi}{U}\right)\right]\right\} \tag{7}$$

where $\theta \equiv (T_o - T_\infty)/(T_o - T_\infty) = 1$.

In reality, equation (7) is more physically correct than equation (5) because it allows for a temperature gradient at the entrance. Outside the entrance, $u(\tau - \frac{\xi}{U}) = 1$, and equation (7) is identical to equation (5). However, within the entrance, where $u[\frac{\alpha}{r^2}(\tau - \frac{\xi}{U})] = 0$, the two equations differ by the term $\gamma(\theta - \theta_o)$; and, as ξ becomes large, T must approach T_o, in which case convection from the side vanishes, as expected.

Equation (7) may be put in dimensionless form by the introduction of the following variables: $\eta = \xi/r$, $Fo = \alpha\tau/r^2$, $Bi = hr/k$, and $Pe = rU/\alpha = (rU\rho/\mu)(c_p\mu/k) = RePr$ where η is the dimensionless distance, Fo is the Fourier modulus, Bi is the Biot number, k is the thermal conductivity of the strand material, Pe is the Peclet number, ρ is the density of the strand material, μ is the viscosity of the strand material, c_p is the specific heat of the strand material, Re is the Reynolds number, and Pr is the Prandtl number. Then, equation (7) becomes

$$\frac{\partial^2\theta}{\partial\eta^2} - 2Bi\theta = \frac{\partial\theta}{\partial Fo} - 2Bi\left[1 - u\left(Fo - \frac{\eta}{Pe}\right)\right] \tag{8}$$

If equation (8) is applied to a solid wire or billet, the Peclet number representation is meaningless. However, Pe is basically a nondimensionalized velocity rU/α.

Two boundary conditions and an initial condition are imposed as follows. Boundary conditions: $Fo > 0$, $\eta = 0$; $\frac{\partial\theta}{\partial\eta} = Bi_e\theta$, where Bi_e is the Biot number at the end; other boundary condition is $\eta \to \infty$; θ is bounded. Initial condition: $Fo = 0$, $\eta = 0$; $\theta = \theta_o = 1$. With this formulation of the analytical model, attention is now directed toward obtaining a solution for this system that will accurately predict the physical phenomenon.

METHOD OF SOLUTION

If the Laplace transform of both sides of equation (8) is taken with respect to Fo (denoting the transform $\mathcal{L}\{\theta\}$ by $\bar{\theta} = \bar{\theta}(\eta, s)$, where s is the transform variable), the result is a linear second-order ordinary differential equation in $\bar{\theta}$ and η.

$$\frac{d^2\bar{\theta}}{d\eta^2} - (2Bi + s)\bar{\theta} = -1 - \frac{2Bi}{s}\left[1 - \exp\left(-\frac{s\eta}{Pe}\right)\right] \tag{9}$$

The complementary solution can be written as

$$\bar{\theta}_c = A(s)\exp\left(\eta\sqrt{2Bi + s}\right) + B(s)\exp\left(-\eta\sqrt{2Bi + s}\right) \tag{10}$$

where A(s) and B(s) are to be determined from boundary conditions. The particular solution is

$$\bar{\theta}_p = C_1(s) + C_2(s)\exp(-s\eta/Pe) \tag{11}$$

The evaluation of the constants from the boundary conditions yields the general solution of the transformed equation

$$\bar{\theta}(\eta, s) = \exp\left(-\eta\sqrt{2Bi + s}\right)\left\{\frac{-2Bi\left(\frac{1}{Pe} + \frac{Bi_e}{s}\right)}{\left(Bi_e + \sqrt{2Bi + s}\right)\left[\left(\frac{s}{Pe}\right)^2 - (2Bi + s)\right]} - \frac{Bi_e}{s\left(Bi_e + \sqrt{2Bi + s}\right)}\right\} + \frac{1}{s}\left\{1 + \frac{2Bi\exp\left(-\frac{s\eta}{Pe}\right)}{\left[\left(\frac{s}{Pe}\right)^2 - (2Bi + s)\right]}\right\} \tag{12}$$

This solution was verified by taking the appropriate derivatives and by substituting them and equation (12) into equation (8). The inversion of equation (12) provides the general solution for the strand system.

The inversion details are omitted for the sake of brevity. The details, although representing a considerable portion of the effort in solving this problem, are generally straightforward and are given in reference 11. The solution is lengthy and involves exponential and complementary error functions. It is written as

$$\theta(\eta, \mathrm{Fo}) = 1 - u\left(\mathrm{Fo} - \frac{\eta}{\mathrm{Pe}}\right) - 2\mathrm{BiPe}\exp(-2\mathrm{BiFo})\left(A_1 + \mathrm{Bi_e PeD_1}\right)\left\{\frac{1}{2}\exp\left(s_1\mathrm{Fo}\right)\left[\frac{1}{\left(\mathrm{Bi_e} + \sqrt{s_1}\right)}\exp\left(-\eta\sqrt{s_1}\right)\right.\right.$$

$$\cdot\ \mathrm{erfc}\left(\frac{\eta}{2\sqrt{\mathrm{Fo}}} - \sqrt{s_1\mathrm{Fo}}\right) + \frac{1}{\left(\mathrm{Bi_e} - \sqrt{s_1}\right)}\exp\left(\eta\sqrt{s_1}\right)\mathrm{erfc}\left(\frac{\eta}{s\sqrt{\mathrm{Fo}}} + \sqrt{s_1\mathrm{Fo}}\right)\Bigg]$$

$$- \left[\frac{\mathrm{Bi_e}}{\mathrm{Bi_e}^2 - s_1}\right]\exp\left(\mathrm{Bi_e}\eta + \mathrm{Bi_e}^2\mathrm{Fo}\right)\mathrm{erfc}\left(\frac{\eta}{2\sqrt{\mathrm{Fo}}} + \mathrm{Bi_e}\sqrt{\mathrm{Fo}}\right)\Bigg\}$$

$$- 2\mathrm{BiPe}\exp(-2\mathrm{BiFo})\left(B_1 + \mathrm{Bi_e PeE_1}\right)\left\{\frac{1}{2}\exp\left(s_2\mathrm{Fo}\right)\left[\frac{1}{\left(\mathrm{Bi_e} + \sqrt{s_2}\right)}\right.\right.$$

$$\cdot\ \exp\left(-\eta\sqrt{s_2}\right)\mathrm{erfc}\left(\frac{\eta}{2\sqrt{\mathrm{Fo}}} - \sqrt{s_2\mathrm{Fo}}\right) + \frac{1}{\left(\mathrm{Bi_e} - \sqrt{s_2}\right)}\exp\left(\eta\sqrt{s_2}\right)$$

$$\cdot\ \mathrm{erfc}\left(\frac{\eta}{2\sqrt{\mathrm{Fo}}} + \sqrt{s_2\mathrm{Fo}}\right)\Bigg] - \frac{\mathrm{Bi_e}}{\left(\mathrm{Bi_e}^2 - s_2\right)}\exp\left(\mathrm{Bi_e}\eta + \mathrm{Bi_e}^2\mathrm{Fo}\right)\mathrm{erfc}\left(\frac{\eta}{2\sqrt{\mathrm{Fo}}}\right.$$

$$\left.\left. + \mathrm{Bi_e}\sqrt{\mathrm{Fo}}\right)\right\} + \left\{2\mathrm{BiPe}^2 D_1 \exp\left[\left(s_1 - 2\mathrm{Bi}\right)\left(\mathrm{Fo} - \frac{\eta}{\mathrm{Pe}}\right)\right]\right.$$

$$\left. + 2\mathrm{BiPe}^2 E_1 \exp\left[\left(s_2 - 2\mathrm{Bi}\right)\left(\mathrm{Fo} - \frac{\eta}{\mathrm{Pe}}\right)\right]\right\} u\left(\mathrm{Fo} - \frac{\eta}{\mathrm{Pe}}\right)$$

where

$$A_1 = \frac{1}{\mathrm{Pe}\left(\mathrm{Pe}^2 + 8\mathrm{Bi}\right)^{\frac{1}{2}}} \tag{14}$$

$$B_1 = -A_1 \tag{15}$$

$$D_1 = \frac{1}{\frac{Pe}{2}\left(Pe^2 + 8Bi\right)^{\frac{1}{2}}\left[Pe^2 + Pe\left(Pe^2 + 8Bi\right)^{\frac{1}{2}}\right]} \tag{16}$$

$$E_1 = \frac{1}{\frac{Pe}{2}\left(Pe^2 + 8Bi\right)^{\frac{1}{2}}\left[Pe^2 - Pe\left(Pe^2 + 8Bi\right)^{\frac{1}{2}}\right]} \tag{17}$$

and where s_1 and s_2 are roots of a quadratic given by

$$s_{1,2} = \frac{1}{2}\left\{\left(4Bi + Pe^2\right) \pm \left[\left(4Bi + Pe^2\right)^2 - 16Bi^2\right]^{\frac{1}{2}}\right\} \tag{18}$$

The ultimate check of correctness for the general solution was performed successfully by taking the appropriate partial derivatives from equation (13) and substituting them into the governing differential equation (8).

APPLICATION OF THE SOLUTION

The solution, equation (13), yields θ as a function of η and Fo, with Bi, Bi_e, and Pe as parameters. The Biot numbers Bi and Bi_e represent the ratio of internal to external resistance to heat transfer and must be kept quite low if the neglect of radial temperature gradients is to hold. For this investigation, Biot numbers were limited to 0.1 or less.

Equation (13) is applicable for all times; however, as time (Fo) becomes large, arguments in the solution become correspondingly large. If these terms are separated from the overall solution and are designated for convenience θ_2, then

$$\theta_2 = 2BiPeD_1 \exp\left[\left(s_1 - 2Bi\right)Fo\right]\left\{-\left(\frac{A_1}{D_1} + Bi_e Pe\right)\frac{1}{2}\frac{\exp\left(-\eta\sqrt{s_1}\right)}{\left(Bi_e + \sqrt{s_1}\right)}\right.$$

$$\left. \cdot \operatorname{erfc}\left(\frac{\eta}{2\sqrt{Fo}} - \sqrt{s_1 Fo}\right) + Pe \exp\left[-\left(s_1 - 2Bi\right)\frac{\eta}{Pe}\right]\left[u\left(Fo - \frac{\eta}{Pe}\right)\right]\right\} \tag{19}$$

The remainder of equation (13) would then be called θ_1, so that $\theta = \theta_1 + \theta_2$. This grouping of terms eliminates complications caused by machine limitations at large times. Generally, as $Fo \to \infty$, the exponential functions involving Fo become larger. It can be shown that for long times, approaching steady state, θ_2 becomes of negligible significance. A brief demonstration of this is given in appendix B.

Figure 4 shows the end temperature ratio of the strand $\theta(0, Fo)$ for a Biot number of 10^{-3} and for various Peclet numbers. The lower the Peclet number, the longer the time required for the end to cool to essentially the coolant temperature. Initially, this fact seems contrary to intuition; however, the effect of axial conduction is being demonstrated here. Low Peclet numbers correspond to strands that move away from the reservoir slowly. Axial conduction is effective in these cases, and the strand cools more slowly. Figure 4 also shows that high Peclet numbers (Pe > 1) have little effect. This situation corresponds to the case of a more rapidly moving strand where axial conduction does not contribute so heavily.

For small metal jets or strands, the Peclet number is fairly high except for very slow moving strands. Figures 5 and 6 show the cooling results for the leading edge for two Biot numbers smaller than that of figure 4. When the leading edge approaches the temperature of the coolant ($\theta = 0$), no further cooling of the strand past that point occurs. Essentially, figures 4, 5, and 6 yield the Fo at the time when the strand approaches a steady-state condition. At this point, the temperature profiles in the strand undergo no further change.

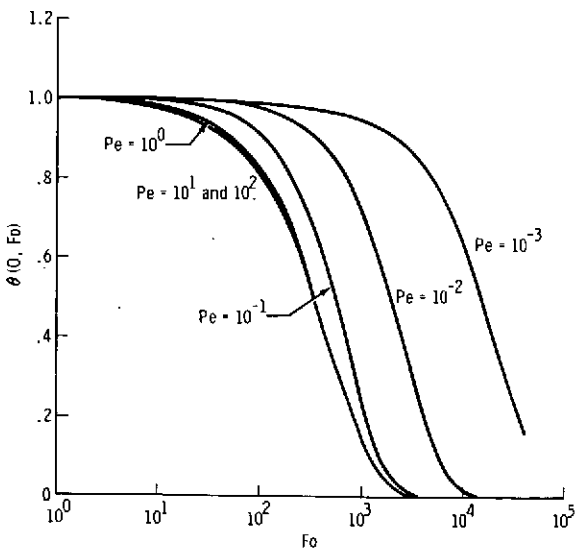

Figure 4.- Cooling of the end of the strand: Bi = 10^{-3}.

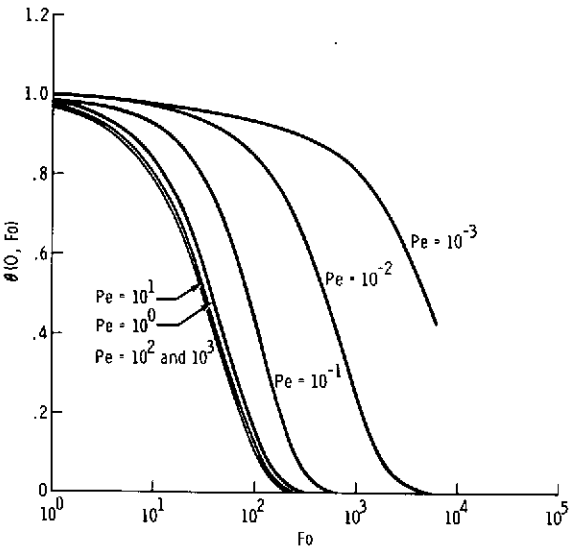

Figure 5.- Cooling of the end of the strand: Bi = 10^{-2}.

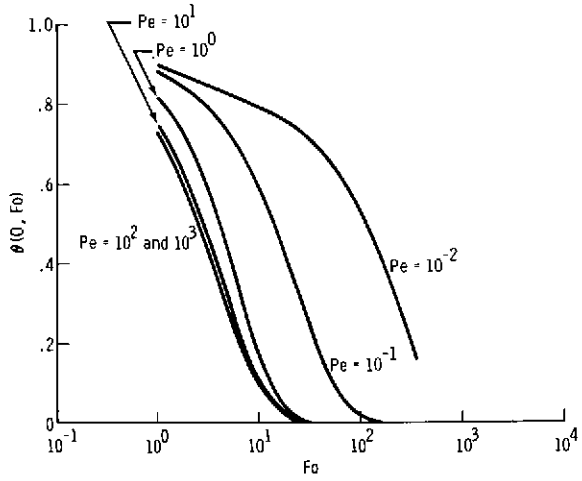

Figure 6.- Cooling of the end of the strand: $Bi = 10^{-1}$.

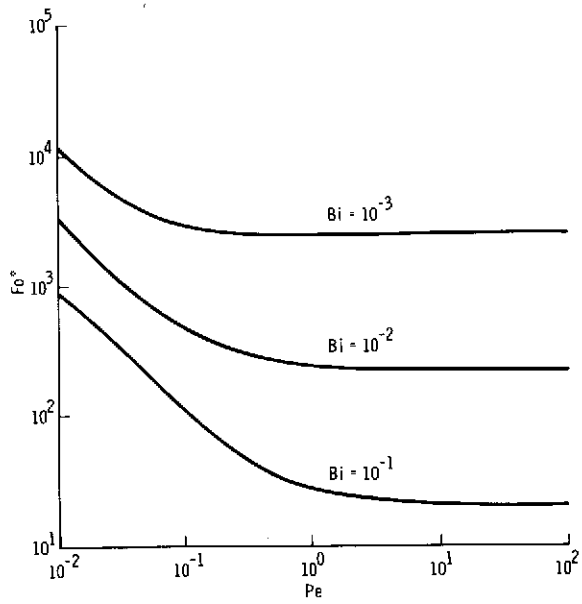

Figure 7.- Time required to reach steady state for low-Biot-number strands.

The time to steady state Fo* is determined by

$$\theta(\eta, \text{Fo}, \text{Bi}, \text{Pe}) = \theta(0, \text{Fo}^*, \text{Bi}, \text{Pe}) = 0 \tag{20}$$

In actuality, θ only approaches zero asymptotically; therefore, Fo* was determined as the time required for θ to reach $\theta = 0.01$. Figure 7 shows the steady-state time plotted with Bi as a parameter for a range of Pe that will encompass most situations of practical interest. The figure shows that Fo* decreases with increasing Bi but increases with decreasing Pe for $\text{Pe} < 10$. For $\text{Pe} > 10$, the Fo* is essentially constant, indicating the same effect as shown in figure 4 but in a slightly different manner; that is, relatively large Pe has a negligibly small effect on the cooling rate of the strand. Clearly, the Bi could be a function of Pe, but that interdependence was not included in this investigation.

However, the Pe does have a bearing on the length of the strand when it reaches a steady-state condition. The product PeFo* gives the steady-state distance η^* as the strand tip approaches the coolant temperature. Figure 8 shows the variation in steady-state length for a wide range of Pe. This figure illustrates that, if Bi and Pe are known for a strand, the nondimensional η^* can be found easily.

Figures 9, 10, and 11 show how the temperature profiles develop as time proceeds for strands with $\text{Pe} = 10^2$. The distance scale is normalized versus the length of the strand at a particular Fo. For example, in figure 9, the plots for Fo of 5×10^1, 5×10^2, and 10^3 are for $\text{Fo} < \text{Fo}^*$; and the curve for $\text{Fo} = 10^4$ is for $\text{Fo} > \text{Fo}^*$.

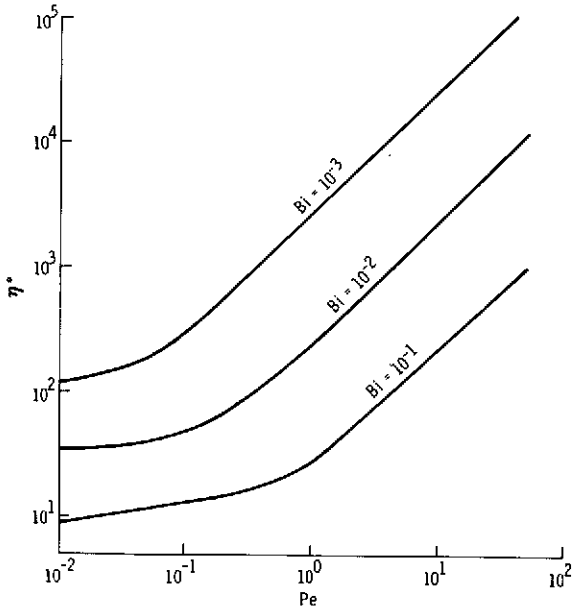

Figure 8.- Length of strand required for steady state.

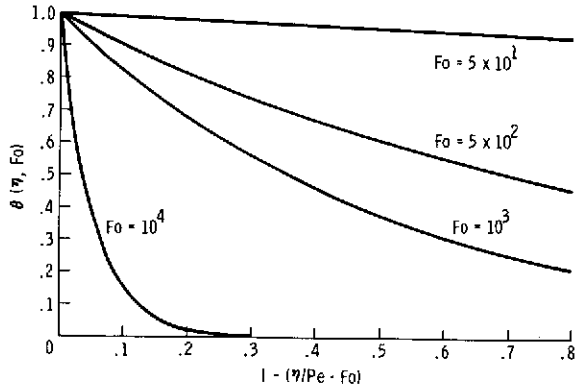

Figure 9.- Development of temperature profile: Bi = 10^{-3}, Pe = 10^2.

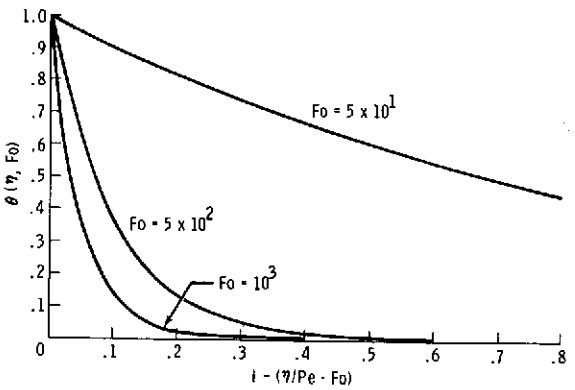

Figure 10.- Development of temperature profile: Bi = 10^{-2}, Pe = 10^2.

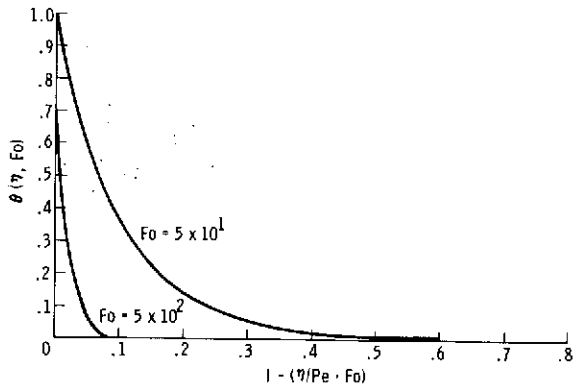

Figure 11.- Development of temperature profile: Bi = 10^{-1}, Pe = 10^2.

The test of any theoretical result is a comparison with experimental results. Acierno et al. (ref. 2) have obtained temperature profiles for polyethylene fibers at 453° to 473° K (180° to 200° C) being pulled from an extruder into stagnant air at 293° to 298° K (20° to 25° C). The conditions for this test do not exactly match those of the theory developed in this report; for example, the strand was being extended and the diameter decreased as the extension took place. Therefore, the velocity and diameter of the strand are functions of the distance from the spinneret. Another difference is possibly due to the variation in thermal conductivity in the radial direction as a result

of radial temperature gradients. Even with these differences, axial temperature distributions computed from the theory of this report show an excellent comparison in shape with those measured by Acierno, indicating that the theory is correct, at least in its dependence on basic parameters of the system.

Bradley (ref. 12) undertook a companion experimental study to this theoretical study. He studied the cooling characteristics of a 0.159-cm-diameter (1/16-inch-diameter) molten metal jet in distilled water. The effects of drag caused the jet to be slowed as it penetrated into the liquid, resulting in considerable waviness in the jet. Direct temperature measurements along the jet could not be obtained, but in some cases behavior was observed that compares well with the theoretical results of this analysis. Bradley noted that solidification of the jet occurred at a fixed axial location from the injection nozzle, after the jet had penetrated the cooling bath considerably. Under similar conditions, the theory of this investigation predicts that the temperature at which solidification would begin is reached at a constant axial distance from the reservoir.

Data that could be compared directly to the theory were not found. Complete verification of the theoretical formulation must await such results. Meanwhile, work is being conducted to obtain data by means of an apparatus involving the passage of a solid wire through a cooling region.

CONCLUDING REMARKS

A mathematical model was developed to describe the heat transfer characteristics of a hot jet or strand emerging into a surrounding coolant. A closed-form analytical solution of the governing partial differential equation was obtained for a circular strand of constant efflux velocity and constant (average) heat transfer coefficient on its sides. Using this model, the various parameters governing the thermal behavior of the strand were investigated. Although a limited comparison with experimental data was made, more experimental data are needed with which to compare the theory.

The complexity of determining an adequate heat transfer coefficient on the strand was illustrated by a simplified analysis consisting of an extension of previous work to include several effects that would be present in most applications of interest. In the model, it was necessary to use an average heat transfer coefficient. The effects of variations in this coefficient were investigated parametrically. For a specific physical application, an initial average heat transfer coefficient can be computed, and this average coefficient can then be used in the model to determine the thermal performance of the strand. With this information, the computation for the heat transfer coefficient can be refined. This procedure can be repeated as many times as necessary until a sufficiently accurate average overall heat transfer coefficient for the strand system is obtained.

The principal limitations of the analysis are summarized as follows. For the case of a freely moving strand, the assumption of a stable axisymmetric strand at constant velocity does not provide for velocity retardation or deformation of strand material as it penetrates the coolant. This limitation is not applicable in the case of a fiber or strand being pulled through the coolant at a constant velocity. These effects perhaps

would not be significant for the small times of interest for fast-cooling small strands because stable film boiling would soon give way to transition and subsequent nucleate boiling, which is beyond the realm of this report. However, if the temperature at which transition occurs is known, then the solution will provide a prediction for the time required for a strand to experience transition. The neglection of a radial temperature gradient within the strand has the effect of limiting the application to materials of high thermal conductivity or to strands of small radius. The assumption of a constant average heat transfer coefficient necessarily implies that an accurate value of this coefficient be computed, and this computation is the one that most severely limits the analysis for any given application.

Therefore, areas of further study should concentrate on striving to eliminate the previously mentioned limitations so that the scope of application of this effort may be widened. The inclusion of a radial temperature gradient within the strand leads to the consideration of Bessel functions. It would allow for more accurate analysis of strands with large radii. Further work is needed in the area of determining the heat transfer coefficient for this geometry. The uniform-temperature assumption presents a significant limitation, and much work is needed here, both experimental and analytical. In particular, hydrodynamic aspects and their effect on the heat transfer process should be investigated in greater detail. The effects of velocity retardation and deformation should be studied. Perhaps such a study could lead to deformation predictions and to the determination of a time-varying heat transfer coefficient at the leading edge.

Lyndon B. Johnson Space Center
National Aeronautics and Space Administration
Houston, Texas, December 10, 1973
981-10-00-00-72

APPENDIX A

DETERMINATION OF HEAT TRANSFER COEFFICIENT

In this appendix, a simplified analytical approach directed at calculating an average heat transfer coefficient for forced-convection film boiling on the strand sides is presented. Although some of the same symbols that were used in the text will be used in this appendix, many of the meanings are different.

SYMBOLS

c_p specific heat at constant pressure

F dimensionless liquid stream function, defined in equation (A14)

f dimensionless vapor stream function, defined in equation (A11)

h overall local heat transfer coefficient, $q''/(T_w - T_\infty)$

h_{fg} latent heat of vaporization

h_r local radiation heat transfer coefficient, defined in equation (A22)

k thermal conductivity of vapor

$\dot{m}$ mass flow rate at interface

Nu overall local Nusselt number, hx/k

Nu_r radiation Nusselt number

Pr Prandtl number, $c_p \mu/k$

q''_c conduction heat transfer

q''_r radiation heat transfer

Re Reynolds number, Ux/ν_L

T static temperature

T_{sat} coolant saturation temperature

T_w wall temperature

T_∞ free-stream temperature

U free-stream velocity

u velocity component in x direction

v velocity component in y direction

x position coordinate

y position coordinate

β parameter for subcooled boiling, defined in equation (A43)

δ vapor film thickness

ϵ_L thermal emissivity of liquid coolant

ϵ_w thermal emissivity of strand material

η vapor similarity variable, defined in equation (A10)

η_δ dimensionless vapor film thickness

θ dimensionless temperature for vapor, defined in equation (A12)

θ_L dimensionless temperature for liquid, defined in equation (A33)

κ thermal diffusivity

λ^* modified latent heat, defined in equation (A23)

μ absolute viscosity

ν kinematic viscosity

ξ liquid similarity variable, defined in equation (A13)

ρ density

ψ stream function for vapor

ψ_L stream function for liquid

HEAT TRANSFER COEFFICIENT

Although a constant (average) heat transfer coefficient (which is treated parametrically) is used in obtaining the solution of the governing heat transfer equation (18) of the strand system, the overall coefficient of heat transfer on the sides of the jet is, in general, a complex function of the thermodynamics and hydrodynamics of the flow system with its associated boundary-layer interactions. Other factors that complicate the analysis are radiation effects and subcooled boiling.

An analysis to determine heat transfer and friction characteristics during forced-convection film boiling on a flat plate, neglecting radiation and subcooling effects, was performed by Cess and Sparrow (ref. 7), and their approach is used in the analysis of this appendix; however, unlike the former study, this analysis includes the effects of radiation and subcooled boiling. In applying the flat-plate results to the sides of the jet, the effects of curvature are ignored. The work of Okabe (ref. 13) shows that the incompressible laminar boundary-layer flow along a two-dimensional flat plate is substantially similar to that of axial flow along a circular cylinder near the leading edge, where the ratio of boundary-layer thickness to strand radius is small. Conceptually, the cylindrical surface of the jet is approximated by incremental surface elements such as section AA in figure A-1(a). Figure A-1(b) illustrates the growth of the liquid and vapor boundary layers beginning at the leading edge of the surface element, and also shows the two-dimensional rectangular coordinate system used in the boundary-layer analysis.

So that the governing equations will be analytically tractable, the following assumptions are needed:

1. A stable vapor film exists, with all generated vapor remaining in the film. Also, no interfacial waviness or film instabilities are present.

2. The flow is steady, with negligible gravitational forces.

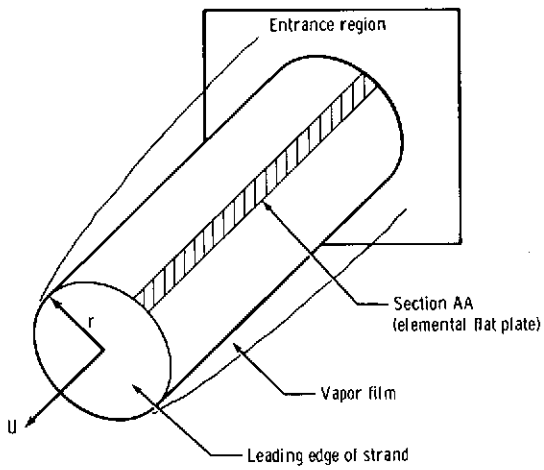

(a) Oblique view of emergent strand, illustrating applicability of flat-plate analysis to an axial surface element.

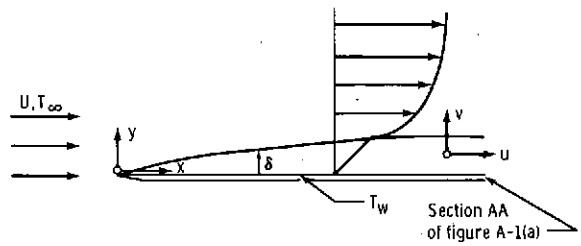

(b) Analytical model for boundary-layer analysis, showing free-stream velocity U relative to emerging flat-plate element of strand.

Figure A-1.- Physical model for calculating heat transfer coefficient on strand sides.

3. The plate surface temperature is uniform. Therefore, the determination of the heat transfer coefficient must be based on an average strand surface temperature, which is not accurately known. This implies an iterative process for obtaining a refined value of the overall heat transfer coefficient.

4. A constant-property vapor is assumed, or a variable-property vapor characterized by $\rho\mu$ = constant, ρk = constant, and Pr = constant (where ρ is density, μ is absolute viscosity, k is the thermal conductivity of vapor, and Pr is the Prandtl number).

5. Inertia forces and energy convection within the vapor film are neglected, and a linear velocity profile is assumed in the vapor layer.

6. The density-viscosity product in the vapor layer is very much smaller than that in the liquid layer; that is, $(\rho\mu) \ll (\rho\mu)_L$.[1]

7. Regarding radiation effects, the vapor layer is assumed to be a nonparticipating gas; that is, absorption and emission within the vapor layer are neglected. This assumption is based on the work of Sparrow (ref. 14) for film boiling in free convection on a vertical flat plate, in which it is concluded that the effects of a radiatively participating vapor on heat transfer are negligible within the parameter range investigated, which includes steam at pressures at least as great as 10 atmospheres.

Because the derivation of the equations is quite lengthy, only a general discussion of the analysis is presented here. More detailed information on the method used is available in the cited references.

The analysis is begun by first considering the coolant fluid to be a saturated liquid. The effects of subcooling are incorporated later. In laminar flow, the governing equations are those of continuity, momentum, and energy. They are expressed as

$$\frac{\partial u}{\partial x} + \frac{\partial v}{\partial y} = 0 \tag{A1}$$

$$u \frac{\partial u}{\partial x} + v \frac{\partial u}{\partial y} = \nu \frac{\partial^2 u}{\partial y^2} \tag{A2}$$

$$u \frac{\partial T}{\partial x} + v \frac{\partial T}{\partial y} = \kappa \frac{\partial^2 T}{\partial y^2} \tag{A3}$$

[1] In this appendix, variables without subscripts refer to the vapor, and the subscript L is used for the liquid.

where u is the velocity of fluid in the x direction, v is the velocity of fluid in the y direction, x and y are position coordinates, ν is the kinematic viscosity, T is the static temperature, and κ is the thermal diffusivity. Although equations (A1), (A2), and (A3) apply to both the liquid and vapor, equation (A3) is not used for the liquid coolant in the preliminary formulation because the temperature in the liquid is assumed to be everywhere constant and equal to the saturation temperature. As written here, the governing equations represent a constant-property vapor. However, as shown in reference 7, for a variable-property vapor adhering to the relations $\rho\mu$ = constant, ρk = constant, and Pr = constant, the final heat transfer and skin friction results are identical to those predicted by the constant-property analysis.

For continuity at the liquid-vapor interface ($y = \delta$, where δ is the vapor film thickness), the tangential velocities, tangential shears, and mass flows that cross the interface are equated for the liquid and vapor.

$$\text{Tangential velocity:} \quad u_L = u \tag{A4}$$

$$\text{Tangential shear:} \quad \mu_L\left(\frac{\partial u}{\partial y}\right)_L = \mu\left(\frac{\partial u}{\partial y}\right) \tag{A5}$$

$$\text{Mass flow crossing interface:} \quad \rho_L\left(u\,\frac{d\delta}{dx} - v\right)_L = \rho\left(u\,\frac{d\delta}{dx} - v\right) \tag{A6}$$

For temperature continuity at the interface, the vapor temperature at the interface must be equal to the liquid temperature; that is,

$$T = T_\infty \quad \text{at} \quad y = \delta \tag{A7}$$

where T_∞ is the free-stream temperature.

Other boundary conditions needed are the conventional ones that apply at the wall and in the free stream.

$$\text{At} \quad y = o, \quad u = v = o \quad \text{and} \quad T = T_w \tag{A8}$$

$$\text{As} \quad y \to \infty, \quad u \to U \tag{A9}$$

where T_w is the wall temperature, and U is the free-stream velocity.

Then, as in reference 7, boundary-layer similarity transformations are introduced, first for the vapor layer in which

$$\eta \equiv \frac{y}{2}\sqrt{\frac{U}{\nu x}} \tag{A10}$$

$$f(\eta) \equiv \frac{\psi}{\sqrt{\nu U x}} \tag{A11}$$

$$\theta(\eta) \equiv \frac{T - T_\infty}{T_w - T_\infty} \tag{A12}$$

where η is the vapor similarity variable, f is the dimensionless vapor stream function, ψ is the stream function, and θ is the dimensionless temperature. Then, for the liquid layer,

$$\xi \equiv \frac{y - \delta}{2}\sqrt{\frac{U}{\nu_L x}} \tag{A13}$$

$$F(\xi) \equiv \frac{\psi_L}{\sqrt{\nu_L U x}} \tag{A14}$$

where ξ is the liquid similarity variable, F is the dimensionless liquid stream function, and ψ_L is the stream function.

The similarity parameters are used to transform the governing partial differential equations into the following ordinary differential equations (ref. 15).

$$f''' + ff'' = 0 \tag{A15}$$

$$\theta'' + (Pr)f\theta' = 0 \tag{A16}$$

$$F''' + FF'' = 0 \tag{A17}$$

where the primes denote differentiation with respect to η in equations (A15) and (A16), and with respect to ξ in equation (A17).

Next, transformation of the boundary conditions, equations (A4) to (A9), results in the following conditions, first at the heated surface

$$f(0) = f'(0) = 0 \quad \text{and} \quad \theta(0) = 1 \tag{A18}$$

then at the liquid-vapor interface

$$\left.\begin{aligned} F(0) &= \left[\frac{\rho\mu}{(\rho\mu)_L}\right]^{1/2} f(\eta_\delta); \quad F'(0) = f'(\eta_\delta) \\ F''(0) &= \left[\frac{\rho\mu}{(\rho\mu)_L}\right]^{1/2} f''(\eta_\delta); \quad \theta(\eta_\delta) = 0 \end{aligned}\right\} \tag{A19}$$

where η_δ is the dimensionless vapor film thickness, and finally in the free stream

$$F' \to 2 \quad \text{as} \quad \xi \to \infty \tag{A20}$$

Equations (A15) to (A20) form the complete set of governing equations for the transformed problem. Knowing the fluid properties, the three unknowns f, F, and θ can be obtained by solution of equations (A15) to (A17) if something is known about η_δ. This information is obtained by writing an energy balance at the interface. At this point, a departure from the approach of Cess and Sparrow (ref. 7) is necessary in order to include radiation effects. When the sum of the conduction and radiation terms at the interface is equated to the heat required to evaporate the liquid, the energy balance becomes

$$-k\frac{\partial T}{\partial y} + h_r(T_w - T_{sat}) = \dot{m}\lambda^* \tag{A21}$$

where h_r is the local radiation heat transfer coefficient, T_{sat} is the coolant saturation temperature, $\dot{m}$ is the mass flow rate at the interface, and λ^* is the modified latent heat. In equation (A21),

$$h_r \equiv \frac{\sigma(T_w^4 - T_{sat}^4)}{(T_w - T_{sat})}\left(\frac{\epsilon_L\epsilon_w}{\epsilon_L + \epsilon_w - \epsilon_L\epsilon_w}\right) \tag{A22}$$

and

$$\lambda^* \equiv h_{fg}\left[1 + \frac{0.84\, c_p\left(T_w - T_{sat}\right)}{h_{fg} \cdot Pr}\right] \tag{A23}$$

where ϵ_L is the thermal emissivity of the liquid coolant, ϵ_w is the thermal emissivity of the strand material, h_{fg} is the latent heat of evaporation, and c_p is the specific heat at constant pressure.

The radiation heat transfer coefficient (eq. (A22)) takes the stated form with the assumption that the vapor layer is very thin; and because of this, the radiant interchange between a surface element and the liquid occurs between locations that are essentially opposite one another. For this reason, the nonparallelism of the surface and the interface will not affect the local radiant heat transfer, and, if curvature of the strand sides is neglected, then the configuration factor for two parallel planes can be used.

The λ^* as defined in equation (A23) is used in equation (A21) because it has been shown (ref. 14) that the effects of the vapor inertia forces and of superheating essentially can be eliminated from the problem by defining such a modified latent heat of vaporization in terms of the actual latent heat h_{fg}, the temperature difference $T_w - T_{sat}$, and the vapor properties.

Transforming the right side of equation (A6) for $\dot{m}$ into the new variables and evaluating the gradient at the interface, equation (A21) becomes

$$\left(\frac{c_p \Delta T}{\lambda^*}\right) = \frac{(Pr) f\left(\eta_\delta\right) (Re)^{1/2}}{\left[2Nu_r\left(\frac{\nu}{\nu_L}\right)^{1/2} - \theta'\left(\eta_\delta\right)(Re)^{1/2}\right]} \tag{A24}$$

where Re is the Reynolds number, and Nu is the overall local Nusselt number. The parameter η_δ is thus replaced by the dimensionless parameter $c_p \Delta T/\lambda^*$, which is a function only of physical properties and of the temperature difference $\Delta T = T_w - T_{sat}$.

According to Cess and Sparrow (ref. 7), certain simplifications can be made at this point that permit an easy yet accurate solution for the range of parameters encountered in the applications of interest for this investigation. The first simplification is to neglect inertia forces and energy convection within the vapor film. This results in simplification of equations (A15) and (A16) to

$$f''' = 0 \quad \text{and} \quad \theta'' = 0 \tag{A25}$$

the solutions of which, together with the boundary conditions at the interface and plate surface, allow the determination of $f(\eta_\delta)$ and $\theta'(\eta_\delta)$, from which equation (A24) becomes

$$\left[\frac{c_p \Delta T}{\lambda^*(Pr)}\right]\left[\frac{(\rho\mu)_L}{\rho\mu}\right] = \frac{\frac{1}{2}\frac{F'^2(0)}{F''(0)}(Re)^{1/2}}{\left\{2Nu_r\left[\frac{\rho\mu}{(\rho\mu)_L}\right]^{-1/2} + \frac{F''(0)}{F'(0)}(Re)^{1/2}\right\}} \tag{A26}$$

Equation (A26) reduces to Cess and Sparrow's (ref. 7) equation (18) when radiation effects are negligible, with the exception that the modified latent heat λ^* is used instead of h_{fg}.

The velocity problem in the liquid is identical to that solved by Cess and Sparrow (ref. 7) with the aid of assumption 6 mentioned previously; therefore, it need not be repeated here. The method of solution relies on the adaptation of the Emmons-Leigh table of solutions (ref. 16) for the problem of blowing or suction normal to a flat plate. (See reference 7.) Several values for the derivatives $F'(0)$ and $F''(0)$ are shown in table A-I for use in equation (A26) and subsequently.

TABLE A-I. - VALUES OF DERIVATIVES AND RELATED FUNCTIONS USED IN THE VELOCITY PROBLEM FOR THE LIQUID

$F'(0)$	$F''(0)$	$\frac{F'^2(0)}{F''(0)}$	$\frac{F''(0)}{F'(0)}$
0.000	1.328	0	∞
.491	1.218	.198	2.48
.668	1.135	.393	1.70
.787	1.067	.580	1.36
.877	1.011	.761	1.15
1.005	.926	1.091	.921
1.117	.842	1.482	.754
1.175	.799	1.728	.680
1.20	.787	1.830	.656
1.30	.700	2.414	.539
1.40	.612	3.203	.437
1.50	.519	4.335	.346
1.60	.423	6.052	.264
1.70	.322	8.975	.189
1.80	.218	14.863	.121
1.90	.111	32.523	.0584
1.92	.0904	40.779	.0471
1.94	.0678	55.510	.0349
1.96	.0451	85.180	.0230
1.98	.0226	173.469	.0114
2.00	.00	∞	.00

The local heat transfer from the strand sides is that caused by conduction (q''_c) through the vapor film and by radiation (q''_r) from the surface, and the local heat transfer rate per unit area (q'') can be expressed as

$$q'' = q''_c + q''_r$$

$$= \frac{k}{2}\sqrt{\frac{U}{\nu x}} \cdot \Delta T \cdot \left[\frac{(\rho\mu)_L}{\rho\mu}\right]^{1/2} \frac{F''(0)}{F'(0)} + h_r \Delta T \qquad \text{(A27)}$$

where the conduction term is that derived by Cess and Sparrow, and the radiation coefficient is as defined in equation (A22). The overall local heat transfer coefficient h is defined as

$$h \equiv \frac{q''}{\Delta T} \qquad \text{(A28)}$$

Therefore, division of both sides of equation (A27) by ΔT yields the desired expression for h.

$$h = \frac{k}{2}\sqrt{\frac{U}{\nu x}}\left[\frac{(\rho\mu)_L}{\rho\mu}\right]^{1/2} \frac{F''(0)}{F'(0)} + h_r \qquad \text{(A29)}$$

Using the definitions from the nomenclature for the combined radiation-conduction Nusselt number, the radiation Nusselt number Nu_r, and the Reynolds number, an expression is obtained for the Nusselt number caused by combined radiation-conduction.

$$\frac{Nu}{(Re)^{1/2}}\left(\frac{\mu}{\mu_L}\right) = \frac{1}{2}\frac{F''(0)}{F'(0)} + \frac{Nu_r}{(Re)^{1/2}}\left(\frac{\mu}{\mu_L}\right) \qquad \text{(A30)}$$

Then, if equation (A26) is rearranged into the same dimensionless parameters as equation (A30)

$$\left[\frac{c_p \Delta T}{\lambda^*(Pr)}\right]\left[\frac{(\rho\mu)_L}{\rho\mu}\right] = \frac{\frac{1}{2}\frac{F'^2(0)}{F''(0)}}{\left[\frac{2(Nu)_r}{(Re)^{1/2}}\left(\frac{\mu}{\mu_L}\right) + \frac{F''(0)}{F'(0)}\right]} \qquad \text{(A31)}$$

Equations (A30) and (A31) can then be used in conjunction with table A-I to produce the plot of figure A-2, in which the influence of radiation is indicated. When radiation effects are negligible, the bottom curve shown is identical to that obtained by Cess and Sparrow.

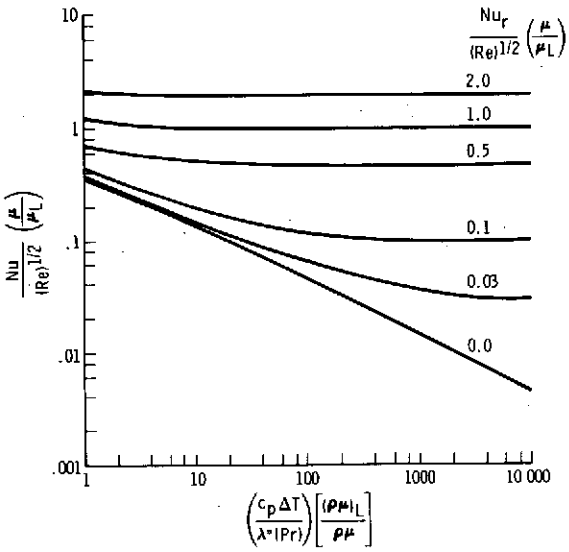

Figure A-2.- Effect of radiation on overall heat transfer.

The analysis will now be extended to include subcooled boiling. Where previously it had been assumed that the coolant liquid was saturated throughout (that is, $T_\infty = T_{sat}$), it must now be specified that $T_\infty < T_{sat}$, but at $y = \delta$ for any x, $T(x, \delta) = T_{sat}$. An additional equation, the energy equation for the liquid, is needed.

$$u \frac{\partial T}{\partial x} + v \frac{\partial T}{\partial y} = \kappa_L \frac{\partial^2 T}{\partial y^2} \qquad (A32)$$

By defining the dimensionless parameter

$$\theta_L \equiv \frac{T - T_\infty}{T_{sat} - T_\infty} \qquad (A33)$$

where θ_L is the dimensionless temperature, and by recalling the previous parameters for the liquid layer

$$\xi \equiv \frac{y - \delta}{2} \sqrt{\frac{U}{\nu_L x}} \qquad (A13)$$

$$F(\xi) \equiv \frac{\psi_L}{\sqrt{\nu_L U x}} \qquad (A14)$$

on taking appropriate derivatives, equation (A32) is transformed into the following ordinary differential equation

$$\frac{d^2 \theta_L}{d\xi^2} + (Pr)_L F(\xi) \frac{d\theta_L}{d\xi} = 0 \quad (\xi \geq 0) \qquad (A34)$$

or

$$\theta_L'' + (Pr)_L F \theta_L' = 0 \quad (\xi \geq 0) \tag{A35}$$

where the primes denote differentiation with respect to ξ. The necessary boundary conditions are for any x

$$\theta_L(0) = 1 \tag{A36}$$

and

$$\lim_{y \to \infty} \theta_L(y) = 0 \tag{A37}$$

Cess and Sparrow (ref. 17) have developed special relations for the temperature gradient at the edge of the boundary layer for three liquid Prandtl number regions.

$$\theta_L'(0) = -2\sqrt{\frac{(Pr)_L}{\pi}} \quad \text{(low liquid Prandtl number)} \tag{A38}$$

$$\theta_L'(0) = \frac{-F''(0)}{2 - F'(0)} \quad \text{(liquid Prandtl number unity)} \tag{A39}$$

$$\theta_L'(0) = -\sqrt{\frac{2(Pr)_L F'(0)}{\pi}} \quad \text{(high liquid Prandtl number)} \tag{A40}$$

If an energy balance is written at the liquid-vapor interface ($y = \delta$ or $\xi = 0$), it can be reasoned that the energy convected by the vapor and radiated from the jet surface goes into coolant evaporation and energy convected by the liquid at the interface; thus

$$-k\left(\frac{\partial T}{\partial y}\right) + h_r\left(T_w - T_{sat}\right) = \dot{m}\lambda^* - k_L\left(\frac{\partial T}{\partial y}\right)_L \tag{A41}$$

If the gradients in the liquid and vapor layers are evaluated at the interface in terms of the transform variables, equation (A41) becomes

$$\left[\frac{c_p \Delta T}{\lambda^*(Pr)}\right] = \frac{\frac{1}{2}\frac{F'^2(0)}{F''(0)}}{\frac{2(Nu_r)}{(Re)^{1/2}}\left(\frac{\mu}{\mu_L}\right) + \frac{F''(0)}{F'(0)} + \beta\theta_L'(0)} \tag{A42}$$

where β is a parameter for subcooled boiling and is defined as

$$\beta \equiv \left[\frac{(Pr)}{(Pr)_L}\right]\left(\frac{c_{p_L} \Delta\tilde{T}}{c_p \Delta T}\right) \tag{A43}$$

where

$$\Delta\tilde{T} \equiv T_{sat} - T_\infty \tag{A44}$$

Equation (A42) is used in conjunction with equations (A38), (A39) or (A40), and equation (A30). Equation (A30) is still valid because heat is transferred from the strand surface both by vapor convection and by radiation, irrespective of subcooled boiling.

APPENDIX B

SOLUTION SIMPLIFICATION FOR LARGE TIMES

It can be easily shown that

$$s_1 = \left(\frac{s_1 - 2Bi}{Pe}\right)^2 \tag{B1}$$

Then equation (19) of the text can be written, using equation (B1), as

$$\theta_2 = 2BiPeD_1 \exp\left[\left(s_1 - 2Bi\right)\left(Fo - \frac{\eta}{Pe}\right)\right]\left\{\left[u\left(Fo - \frac{\eta}{Pe}\right)\right]Pe - \left(\frac{A_1}{D_1} + Bi_e Pe\right)\left(\frac{1}{Bi_e + \sqrt{s_1}}\right)\frac{1}{2}\,\mathrm{erfc}\left(\frac{\eta}{2\sqrt{Fo}} - \sqrt{s_1 Fo}\right)\right\} \tag{B2}$$

It also can be shown that

$$\frac{2BiPe\left(\frac{A_1}{D_1} + Bi_e Pe\right)}{Bi_e + \sqrt{s_1}} = 2BiPe^2 \tag{B3}$$

and because

$$\mathrm{erfc}(-x) = 2 - \mathrm{erfc}(x) \tag{B4}$$

equation (B2) may be written as

$$\theta_2 = 2BiPe^2 D_1 \exp\left[\left(s_1 - 2Bi\right)\left(Fo - \frac{\eta}{Pe}\right)\right]\left[\frac{1}{2}\,\mathrm{erfc}\left(\sqrt{s_1 Fo} - \frac{\eta}{2\sqrt{Fo}}\right) + u\left(Fo - \frac{\eta}{Pe}\right) - 1\right] \tag{B5}$$

In the region of interest, that is, where $\eta < PeFo$,

$$u(Fo - \eta/Pe) - 1 = 0 \tag{B6}$$

and presents no problem. The remaining part of equation (B5) as $Fo \to \infty$ now must be examined. First, the square of the complementary error function argument is considered; that is,

$$\left(\sqrt{s_1 Fo} - \frac{\eta}{2\sqrt{Fo}}\right)^2 = \left(s_1 - 2Bi\right)\left(Fo - \frac{\eta}{Pe}\right) + \left(\frac{\eta^2}{4Fo} + 2BiFo\right) \tag{B7}$$

where equation (B1) is used again. It is possible to write

$$\exp\left[\left(s_1 - 2Bi\right)\left(Fo - \frac{\eta}{Pe}\right)\right] = \exp\left[-\left(2BiFo + \frac{\eta^2}{4Fo}\right)\right]\exp\left[\left(\sqrt{s_1 Fo} - \frac{\eta}{2\sqrt{Fo}}\right)^2\right] \tag{B8}$$

If

$$z = \left(\sqrt{s_1 Fo} - \frac{\eta}{2\sqrt{Fo}}\right) \tag{B9}$$

then equation (B5) may be written as

$$\theta_2 = 2BiPe^2 D_1 \exp\left[-\left(2BiFo + \frac{\eta^2}{4Fo}\right)\right]\left[\frac{1}{2}\exp\left(z^2\right)\operatorname{erfc}(z) + u\left(Fo - \frac{\eta}{Pe}\right) - 1\right] \tag{B10}$$

As $Fo \to \infty$, $z \to \infty$. Reference 18 shows that

$$\frac{2}{\sqrt{\pi}}\left(\frac{1}{z + \sqrt{z^2 + 2}}\right) \le \exp\left(z^2\right)\operatorname{erfc}(z) \le \frac{2}{\sqrt{\pi}}\left(\frac{1}{z + \sqrt{z^2 + \frac{4}{\pi}}}\right) \tag{B11}$$

Clearly, as $z \to \infty$, the bounding expressions for $\exp(z^2)\mathrm{erfc}(z)$ approach zero. Consequently, for long times (large Fo), $\theta_2 \to 0$ and $\theta = \theta_1$ only. For cases in which the jet or strand (in this case, probably a bar, wire, or fiber) is issuing continuously into the cooling region, only this portion of the solution need be used.

REFERENCES

1. Witte, L. C.; Cox, J. E.; and Bouvier, J. E.: The Vapor Explosion. Journal of Metals, vol. 22, no. 2, Feb. 1970, pp. 39-44.

2. Acierno, Domenico; Dalton, J. Nelson; Rodriquez, Jorge M.; and White, James L.: Rheological and Heat Transfer Aspects of the Melt Spinning of Monofilament Fibers of Polyethylene and Polystyrene. J. Appl. Polymer Sci., vol. 15, 1971, pp. 2395-2415.

3. Carslaw, H. S.; and Jaeger, J. C.: Operational Methods in Applied Mathematics. Dover Publications, Inc., New York, 1963.

4. Schlichting, Hermann: Boundary Layer Theory. Fourth ed., McGraw-Hill Book Co., Inc., 1960.

5. Witte, L. C.: Film Boiling from a Sphere. I&EC Fundamentals, vol. 7, no. 3, Aug. 1968.

6. Bradfield, W. S.; Barkdoll, R. O.; and Byrne, J. T.: Film Boiling on Hydrodynamic Bodies. Convair Scientific Research Laboratory, Research Note No. 37, Dec. 1960.

7. Cess, R. D.; and Sparrow, E. M.: Film Boiling in a Forced-Convection Boundary-Layer Flow. Trans. ASME, Aug. 1961, pp. 370-376.

8. Kreith, Frank: Principles of Heat Transfer. Fifth printing, International Textbook Co., 1962.

9. McAdams, William H.: Heat Transmission. McGraw-Hill Book Co., Inc., 1954.

10. Brand, Louis: Differential and Difference Equations. John Wiley & Sons, Inc., 1966.

11. Simon, W. E.: Analysis of the Heat Transfer Characteristics of an Emergent Jet. Ph. D. Dissertation, University of Houston, 1970.

12. Bradley, R. H.; and Witte, L. C.: Explosive Interaction of Molten Metals Injected Into Water. Nucl. Sci. Eng., vol. 48, no. 4, Aug. 1972, pp. 387-396.

13. Okabe, J.: Laminar Boundary Layer on a Circular Cylinder in Axial Flow of an Incompressible Fluid. Reports of Research Institute for Applied Mechanics, Kyushu University, Vol. XII, no. 43, 1964, pp. 17-35.

14. Sparrow, E. M.: The Effects of Radiation on Film-Boiling Heat Transfer. Int. J. Heat Mass Transfer, vol. 7, 1964, pp. 229-238.

15. Rosenhead, L., ed.: Laminar Boundary Layers. Oxford at the Clarendon Press, 1963.

16. Emmons, H. W.; and Leigh, D. C.: Tabulation of the Blasius Function with Blowing and Suction. Ministry of Supply, Aeronautical Research Council Technical Report, C. P. No. 157, 1954.

17. Cess, R. D.; and Sparrow, E. M.: Subcooled Forced-Convection Film Boiling on a Flat Plate. J. Heat Transfer, Aug. 1961, pp. 377-379.

18. Abramowitz, Milton; and Stegun, Irene A.: Handbook of Mathematical Tables. National Bureau of Standards, Applied Mathematics Series 55, November 1967, p. 298.

CAT. - 33

NASA-Langley, 1974 S-362